Smart Structures and Systems, *Vol. 23, No. 2 (2019) 195-205*
DOI: https://doi.org/10.12989/sss.2019.23.2.195

Delamination identification of laminated composite plates using measured mode shapes

Yongfeng Xu[1], Da-Ming Chen[2], Weidong Zhu[*2], Guoyi Li[3] and Aditi Chattopadhyay[3]

[1]*Department of Mechanical and Materials Engineering, University of Cincinnati, Cincinnati, OH 45221, USA*
[2]*Department of Mechanical Engineering, University of Maryland, Baltimore County, 1000 Hilltop Circle, Baltimore, MD 21250, USA*
[3]*School for Engineering of Matter, Transport and Energy, Arizona State University, Tempe, AZ 85287, USA*

(Received August 12, 2018, Revised December 20, 2018, Accepted December 30, 2018)

Abstract. An accurate non-model-based method for delamination identification of laminated composite plates is proposed in this work. A weighted mode shape damage index is formulated using squared weighted difference between a measured mode shape of a composite plate with delamination and one from a polynomial that fits the measured mode shape of the composite plate with a proper order. Weighted mode shape damage indices associated with at least two measured mode shapes of the same mode are synthesized to formulate a synthetic mode shape damage index to exclude some false positive identification results due to measurement noise and error. An auxiliary mode shape damage index is proposed to further assist delamination identification, by which some false negative identification results can be excluded and edges of a delamination area can be accurately and completely identified. Both numerical and experimental examples are presented to investigate effectiveness of the proposed method, and it is shown that edges of a delamination area in composite plates can be accurately and completely identified when measured mode shapes are contaminated by measurement noise and error. In the experimental example, identification results of a composite plate with delamination from the proposed method are validated by its C-scan image.

Keywords: laminated composite plate; delamination identification; non-model-based method; mode shape; polynomial fit

1. Introduction

Delamination is one type of structural damage that frequently occurs in laminated composite structures and can be difficult to identify as it is usually hidden from external view. Delamination identification has been a major research topic in the past few decades. Delamination that occurs in relatively small areas in a laminated composite structure can change its local stiffness in neighborhoods of the delamination, which can directly change modal parameters of the structure, including natural frequencies, modal damping ratios and mode shapes (see Valdes *et al.* 1999, Zou *et al.* 2000, Qiao *et al.* 2007, Min *et al.* 2015, Mendrok *et al.* 2015). Effects of delamination on modal parameters of composite structures have been studied with their analytical, semi-analytical and finite element models (see Jafari-Talookolaei *et al.* 2016, Chakraborty *et al*. 2016, Castro and Donadon 2017), and various methods have been developed to identify delamination in composite structures using measured modal parameters.

Damping is known to be more sensitive to occurrence of structural damage than mass and stiffness (see Zou *et al.* 2000), and modal damping ratios can quantify damping of a structure. Modal damping ratios have been found to be the most sensitive modal parameters of a structure to occurrence of damage (see Doebling *et al*. 1996). However, accuracy and repeatability of measured modal damping ratios are vulnerable to variations of environmental conditions such as humidity and temperature (see Zhang *et al.* 2016). Hence, modal damping ratios may not be ideal modal parameters for field identification of delamination. Natural frequencies of a structure can be accurately measured using one or a few measurement points and have been widely used to assist delamination identification in composite structures, since natural frequencies of a composite structure can deviate due to occurrence of delamination (see Pardoen 1989, Valdes *et al*. 1999, Kim and Hwang 2002, Moon *et al.* 2003, Zhang *et al*. 2016, Yang and Oyadiji 2016). It is shown by Pardoen (1989) that occurrence of delamination to a laminated composite beam can cause changes of its natural frequencies, and the changes depend on severity and the location of the delamination. Changes of natural frequencies of a laminated composite beam can indicate severity of its delamination (see Valdes *et al.* 1999). It is shown by Kim and Hwang (2002) that an increase of debonding in a honeycomb sandwich beam progressively reduces its bending stiffness and an increase of severity of the debonding can progressively reduce natural frequencies of the beam. Fatigue damage in laminated composite beams can be identified using a natural frequency reduction model developed by Moon *et al.* (2003). A graphical approach using changes of natural frequencies is proposed to estimate delamination parameters that include its axial and transverse positions (see Zhang *et al.* 2016). Besides

*Corresponding author, Professor.
E-mail: wzhu@umbc.edu

ISSN: 1738-1584 (Print), 1738-1991 (Online)

laminated composite beams, changes of natural frequencies of laminated composite plates depend on severity and locations of delamination (see Yang and Oyadiji 2016).

Besides natural frequencies, mode shapes have been widely used for delamination identification. Damage in a laminated composite structure causes local reduction of its stiffness, which can be reflected as discontinuity in its curvature mode shapes (see Qiao *et al*. 2007, Lestari *et al.* 2007, Yang *et al*. 2016). A technique based on Ritz method to calculate optimal spatial sampling of curvature mode shapes of laminated structures is developed to reduce adverse effects of measurement noise and error and their propagation, and resulting curvature mode shapes can be used for damage identification of laminated composite plates (see Moreno-García *et al.* 2014). Use of generalized fractal dimensions was proposed by Kumar *et al*. (2017) to detect presence of partial delamination in composite laminated beams; it was found that torsional mode shapes were best suited for partial delamination detection in composite beams. Locations and severity of structural damage could be detected by use of curvature-moment and curvature-moment derivative concepts and Bat Algorithm (see Torkzadeh *et al.* 2016). Two previous papers by some of the authors of this work (see Xu and Zhu 2017, Xu *et al.* 2017) use polynomials that fit mode shapes of damaged metal plates to yield mode shapes of undamaged plates for damage identification. Damage can be identified from damage indices that compare mode shapes or curvature mode shapes with those from polynomial fits. An assumption for using a polynomial fit for damage identification is that an undamaged plate is geometrically smooth and made of materials that have no stiffness discontinuities. In order to identify damage in a plate, one needs to obtain damage indices associated with different modes and find neighborhoods with consistently high values of the damage indices. False positive identification results can exist due to measurement noise and error, which exhibits disturbance in the damage indices. False negative identification results can exist when damage has a relatively large size and damage indices associated with different modes can reveal partial information of the damage, such as the position and length of one of its edges. Though the false positive and negative identification results can be alleviated by increasing measurement accuracy and the number of measured mode shapes, one can be confused when damage indices associated with a number of mode shapes are available and some of them provide different damage information.

This work extends the damage identification method in a work by Xu and Zhu (2017), which was applied to identification of damage in the form of thickness reduction in metal plates, to identification of delamination in composite plates using measured mode shapes and polynomial fits. Polynomial fits are used to approximate mode shapes of undamaged composite plates without any of their a priori information. New mode shape damage indices called a synthetic mode shape damage index (sMSDI) and an auxiliary mode shape damage index (aMSDI) are formulated based on a weighted mode shape damage index (wMSDI) to accurately and completely identify lengths and locations of edges of delamination in composite plates, which can exclude false positive identification results caused by measurement noise and error. A laminated composite plate with delamination is manufactured and a finite element model of the composite plate is constructed. Both numerical and experimental investigations are conducted to study effectiveness of the proposed method. In the experimental investigation, an imperfectly clamped boundary condition was applied to the composite plate and identification results are compared with those from its C-scan image.

The remaining part of the paper is outlined as follows. A method to approximate a mode shape of an undamaged composite plate using a polynomial that fits a mode shape of a composite plate with delamination is described in Sec. 2.1, and formulations of wMSDI, sMSDI and aMSDI are described in Sec. 2.2. Effectiveness of the proposed method to identify delamination in a composite plate using sMSDI and aMSDI is numerically investigated in Sec. 3. An experimental investigation is presented in Sec. 4 to validate the proposed method and identification results are compared with those from a C-scan image of the composite plate.

2. Methodology

2.1 Numerical simulation procedure

It is assumed in this work that mode shapes of an undamaged composite plate are unavailable. Such a mode shape at a measurement point with coordinates (x, y) can be well approximated by a polynomial fit (see Xu and Zhu 2017, Xu *et al*. 2017)

$$z^p(x,y) = \sum_{k=0}^{n}\sum_{i=0}^{k} a_{i,k-i} x^i y^{k-i} \tag{1}$$

where n and $a_{i,k-i}$ are the order and coefficients of the polynomial, respectively. The polynomial fits an N-point mode shape of a composite plate with delamination and its coefficients can be obtained by solving an associated set of linear equations

$$\mathbf{V}\mathbf{a} = \mathbf{z} \tag{2}$$

where $\mathbf{z}$ is an N-dimensional mode shape vector to be fit, $\mathbf{V}$ is the $N \times \left(\sum_{p=1}^{n+1} p \right)$-dimensional bivariate Vandermonde matrix

$$\mathbf{V} = \begin{bmatrix} 1 & x_1 & y_1 & \cdots & x_1^n & \cdots & x_1^i y_1^{n-i} & \cdots & y_1^n \\ 1 & x_2 & y_2 & \cdots & x_2^n & \cdots & x_2^i y_2^{n-i} & \cdots & y_2^n \\ \vdots & \vdots & \vdots & \ddots & \vdots & \ddots & \vdots & \ddots & \vdots \\ 1 & x_N & y_N & \cdots & x_N^n & \cdots & x_N^i y_N^{n-i} & \cdots & y_N^n \end{bmatrix} \tag{3}$$

and $\mathbf{a}$ is the $\left(\sum_{p=1}^{n+1} p\right)$-dimensional coefficient vector

$$\mathbf{a}=\begin{bmatrix} a_{0,0} & a_{1,0} & a_{0,1} & \cdots & a_{n,0} & \cdots & a_{i,n-i} & \cdots & a_{0,n} \end{bmatrix}^{\mathrm{T}} \quad (4)$$

The polynomial order n is a parameter that controls the level of approximation of the mode shape from the polynomial fit in Eq. (1) to the mode shape to be fit.

Solving Eq. (2) for $\mathbf{a}$ is equivalent to solving an unconstrained least-squares problem $\min \frac{1}{2}\left\|\mathbf{V}\mathbf{a}^{*}-\mathbf{z}\right\|^{2}$ for an optimum minimizer $\mathbf{a}^{*}$ (see Wright and Nocedal 1999), which is an over-determined problem with $N>\sum_{p=1}^{n+1} p$ in most cases. One can obtain its solution using the singular-value decomposition of $\mathbf{V}$ (see Wright and Nocedal 1999)

$$\mathbf{V}=\mathbf{U}\begin{bmatrix}\mathbf{S}\\ \mathbf{0}\end{bmatrix}\mathbf{W}^{\mathrm{T}} \quad (5)$$

where $\mathbf{U}$ and $\mathbf{W}$ are $N\times N$ and $\left(\sum_{p=1}^{n+1} p\right)\times\left(\sum_{p=1}^{n+1} p\right)$ orthogonal matrices, respectively, and $\mathbf{S}$ is a $\left(\sum_{p=1}^{n+1} p\right)\times\left(\sum_{p=1}^{n+1} p\right)$ diagonal matrix; $\mathbf{a}^{*}$ based on Eq. (5) can be expressed by

$$\mathbf{a}^{*}=\mathbf{W}\mathbf{S}^{-1}\mathbf{U}_{\mathbf{1}}^{\mathrm{T}}\mathbf{z} \quad (6)$$

where $\mathbf{U}_1$ is a matrix formed by the first $\sum_{p=1}^{n+1} p$ columns of $\mathbf{U}$. When n in Eq. (1) is large, $\mathbf{S}$ can be ill-conditioned, which results in a low level of approximation of a mode shape from the polynomial fit. To alleviate ill-conditioning of $\mathbf{S}$, it is proposed that x and y in Eq. (1) be normalized using the "center and scale"' technique (see Cox and Gaudard 2013) before formulating the linear equations in Eq. (2). Normalized coordinates $\tilde{x}$ and $\tilde{y}$ can be expressed by

$$\begin{cases}\tilde{x}=\dfrac{2x-2\bar{x}}{l_1}\\ \tilde{y}=\dfrac{2y-2\bar{y}}{l_2}\end{cases} \quad (7)$$

where $\bar{x}$ and $\bar{y}$ are x- and y-coordinates of the geometric center of the mode shape measurement grid, respectively, and l_1 and l_2 are lengths of the mode shape measurement grid along x- and y-axes, respectively.

An increase of n in the polynomial fit in Eq. (1) can improve its level of approximation of its corresponding mode shape to the mode shape to be fit. To quantify the level of approximation, a fitting index defined by

$$\mathrm{fit}(n)=\frac{\mathrm{RMS}(\mathbf{z})}{\mathrm{RMS}(\mathbf{z})+\mathrm{RMS}(\mathbf{e})}\times 100\% \quad (8)$$

is used, where $\mathrm{RMS}(\cdot)$ denotes the root-mean-square value of a vector and $\mathbf{e}$ is the error vector between the mode shape to be fit and the corresponding one from the current polynomial fit, i.e., $\mathbf{e}=\mathbf{V}\mathbf{a}^{*}-\mathbf{z}$. When the fitting index is close to 100%, the mode shape from the current polynomial fit is almost identical to $\mathbf{z}$; the lower the fitting index, the lower the level of approximation of the mode shape from the current polynomial fit. To determine the proper order of a polynomial fit, a convergence index for a polynomial fit with $n\geq 3$ is defined based on fit

$$\mathrm{con}(n)=\mathrm{fit}(n)-\mathrm{fit}(n-2) \quad (9)$$

A proper value of n is determined to be the minimum value with which con is smaller than a threshold value and the threshold value is proposed to be 0.05% in this work.

2.2 wMSDI, sMSDI and aMSDI

Since a mode shape $\mathbf{Z}^{p}$ from a polynomial that fits a measured mode shape of a composite plate with delamination $\mathbf{Z}^{d}$ can be considered as one of an undamaged composite plate, effects of the delamination on the measured mode shape can be isolated by comparing $\mathbf{Z}^{p}$ and $\mathbf{Z}^{d}$, and wMSDI can be formulated for delamination identification. The wMSDI at a point $\mathbf{p}$ can be expressed by (see Xu and Zhu 2017)

$$\delta(\mathbf{p})=\left\{\sum_{k_1=-M_w}^{M_w}\sum_{k_2=-M_w}^{M_w}\left[\left(\mathbf{Z}^{d}\left(\mathbf{p}_{k_1,k_2}\right)-\mathbf{Z}^{p}\left(\mathbf{p}_{k_1,k_2}\right)\right)\times W_{M_w}(k_1,k_2)\right]\right\}^{2} \quad (10)$$

where $\mathbf{p}_{k_1,k_2}$ is a point with xy-coordinates $\left(x_{\mathbf{p}}+k_1\Delta d, y_{\mathbf{p}}+k_2\Delta d\right)$, in which $x_{\mathbf{p}}$ and $y_{\mathbf{p}}$ are x- and y-coordinates of $\mathbf{p}$, respectively, and Δd is the side length of a square element in a mesh of the measured mode shape, and W_{M_w} is a weight function that can be expressed by

$$W_{M_w}(k_1,k_2)=\mathrm{e}^{-4\left[\left(\frac{k_1}{M_w}\right)^2+\left(\frac{k_2}{M_w}\right)^2\right]} \quad (11)$$

in which M_w is the scale of the weight function, which is an odd integer, and k_1 and k_2 are integer coordinates associated with x- and y-axes of the weight function, respectively, with $k_1,k_2\in\left[-M_w,M_w\right]$. Note that $\mathbf{Z}^{d}$ in Eq. (10) is defined on a mesh of square elements with the same side length. When $\mathbf{Z}^{d}$ is defined on a mesh with non-square elements or square elements with different side

lengths, one needs to interpolate $\mathbf{Z}^d$ for a mode shape on a mesh of square elements with the same side length so that W_{M_w} can have equal weights along x- and y-axes. The weight function W_{M_w} in Eq. (10) resembles a two-dimensional Gaussian filter that can eliminate high-frequency measurement noise in the mode shape difference $\mathbf{Z}^d - \mathbf{Z}^p$, and M_w in Eq. (11) determines the cut-off frequency of the filter: the higher the value of M_w, the lower the cut-off frequency. Delamination can be identified in neighborhoods with consistently high values of wMSDIs associated with different modes.

When measurement noise at low frequencies and measurement error exist in a measured mode shape, δ can include false positive identification results. Without loss of generality, assume such false positive identification results do not persistently occur in areas with no delamination. A sMSDI associated with a mode can be defined by synthesizing δ associated with multiple measured mode shapes of the mode to exclude false positive identification results, and the sMSDI associated with the q-th mode at $\mathbf{p}$ can be expressed by

$$\tilde{\delta}_q(\mathbf{p}) = \left[\Gamma\left(\delta(\mathbf{p})\right)\right]^{\frac{1}{N}} \tag{12}$$

where $\Gamma(\cdot)$ denotes the product of wMSDIs of N available measured mode shapes associated with the mode. wMSDI δ and sMSDI $\tilde{\delta}_q$ can reveal partial spatial information of delamination, such as the position and location of one of its edges, which forms false negative identification results. Hence, one should measure mode shapes associated with different modes in order to obtain more complete delamination identification results. An aMSDI is proposed to assist such a process and can be expressed by

$$\rho(\mathbf{p}) = \begin{cases} 1 & ,\Xi\left|\left(\hat{\delta}_q(\mathbf{p})\right)\right| \geq 1 \\ \left[\Xi\left|\left(\hat{\delta}_q(\mathbf{p})\right)\right|\right]^2 & ,\Xi\left|\left(\hat{\delta}_q(\mathbf{p})\right)\right| < 1 \end{cases} \tag{13}$$

where $|\cdot|$ denotes an absolution value, $\hat{\delta}_q$ is normalized $\tilde{\delta}_q$ so that the maximum absolute value of its entries is one, and $\Xi(\cdot)$ denotes summation over $\hat{\delta}_q$ associated with different modes.

3. Numerical Investigation

A finite element model of a six-laminate $[0^o\ 90^o\ 0^o]_s$ IM-7 fiber reinforced polymer composite plate is constructed to numerically investigate effectiveness of the proposed method. The composite plate has an area of delamination between its third and fourth laminates. Dimensions of the composite plate and delamination area are shown in Fig. 1; the composite plate has a thickness of 0.98 mm. Its mass density is 1545 kg/m^3 and its elasticity matrix is

$$\mathbf{K} = \begin{bmatrix} 286 & 173 & 170.5 & 0 & 0 & 0 \\ 173 & 286 & 170.5 & 0 & 0 & 0 \\ 170.5 & 170.5 & 269.5 & 0 & 0 & 0 \\ 0 & 0 & 0 & 45.3 & 0 & 0 \\ 0 & 0 & 0 & 0 & 45.3 & 0 \\ 0 & 0 & 0 & 0 & 0 & 56.5 \end{bmatrix} \text{GPa} \tag{14}$$

The composite plate has clamped-free-free-free boundary conditions, as shown in Fig. 1, and the clamped boundary is located at its lower boundary. In the finite element model, each laminate is modeled using a total of 140×140 plate elements. Mode shapes of its second and fourth out-of-plane modes, denoted by $\mathbf{Z}^{\text{num},2}$ and $\mathbf{Z}^{\text{num},4}$, respectively, are calculated, as shown in Fig. 2. Natural frequencies corresponding to $\mathbf{Z}^{\text{num},2}$ and $\mathbf{Z}^{\text{num},4}$ are 91.73 and 161.75 Hz, respectively. The mode shapes are normalized so that their maximum amplitudes are one.

Convergence indices con associated with $\mathbf{Z}^{\text{num},2}$ and $\mathbf{Z}^{\text{num},4}$ are calculated, as shown in Figs. 3(a) and 3(b), respectively. Based on the proposed threshold value for con, polynomial orders for $\mathbf{Z}^{\text{num},2}$ and $\mathbf{Z}^{\text{num},4}$ are determined to be $n=9$ and $n=10$, respectively. Mode shapes from polynomials that fit $\mathbf{Z}^{\text{num},2}$ and $\mathbf{Z}^{\text{num},4}$ with the determined orders are shown in Figs. 2(c) and 2(d), respectively. Modal assurance criterion values between mode shapes of the composite plate and those from the polynomial fits are almost 100%, which indicates that they are almost identical to each other, and that between mode shapes of the second and fourth out-of-plane modes is 0.11%, which verifies that they are orthogonal to each other (see Ewins 1984). Weighted mode shape damage indices δ associated with $\mathbf{Z}^{\text{num},2}$ and $\mathbf{Z}^{\text{num},4}$ are shown in Figs. 4(a) and 4(b), respectively. Positions and lengths of upper and lower edges of the delamination area can be accurately identified in δ associated with $\mathbf{Z}^{\text{num},2}$, while those of its left and right edges can be accurately identified in δ associated with $\mathbf{Z}^{\text{num},4}$. Since both

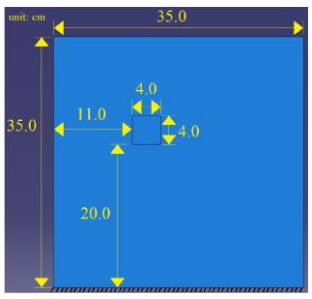

Fig. 1 Dimensions of a six-laminate $[0^o\ 90^o\ 0^o]_s$ IM-7 fiber reinforced polymer composite plate with delamination. The delamination area is a square with the side length of 4.0 cm and located between the third and fourth laminates of the composite plate

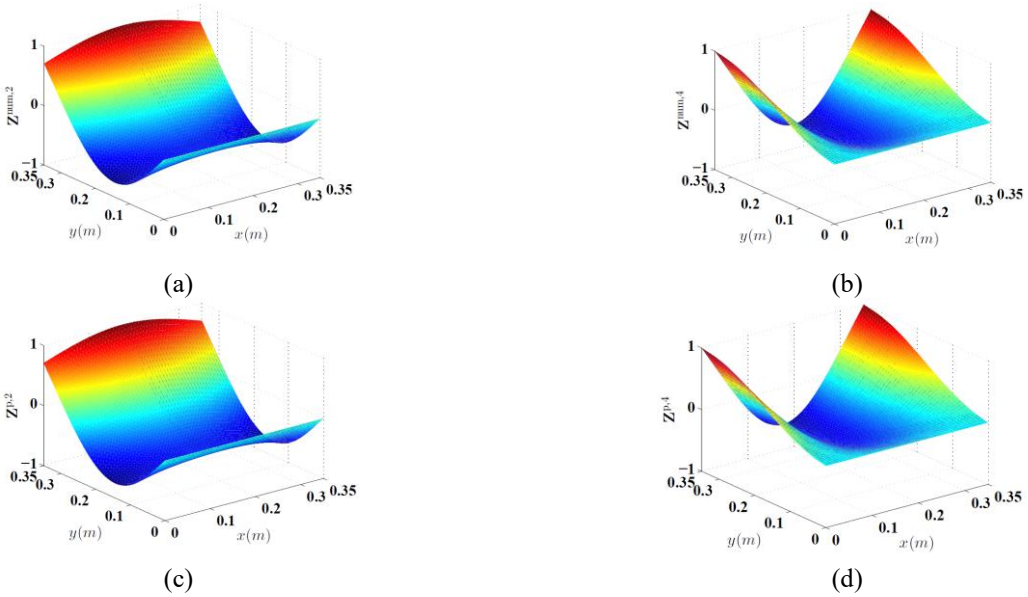

Fig. 2 (a) Mode shape of the second out-of-plane mode of the composite plate, (b) the mode shape of the fourth out-of-plane mode of the composite plate, (c) the mode shape from a polynomial that fits the mode shape in (a) with $n=9$, and (d) the mode shape from a polynomial that fits the mode shape in (b) with $n=10$

Fig. 3 Convergence indices con associated with $\mathbf{Z}^{\text{num},2}$ in Fig. 2(a), and (b) convergence indices associated with $\mathbf{Z}^{\text{num},4}$ in Fig. 2(b)

$\mathbf{Z}^{\text{num},2}$ and $\mathbf{Z}^{\text{num},4}$ are free of measurement noise and error, their δ can be considered as $\tilde{\delta}$. False negative identification results can be observed when only δ associated with either $\mathbf{Z}^{\text{num},2}$ or $\mathbf{Z}^{\text{num},2}$ is considered, since the delamination area is relatively large. aMSDI ρ associated with $\mathbf{Z}^{\text{num},2}$ and $\mathbf{Z}^{\text{num},4}$ is shown in Fig. 4(c), where positions and lengths of the delamination area can be accurately and completely identified.

Hereafter, each mode shape of one mode is measured twice so that there are two measured mode shapes corresponding the mode, and it is assumed that measurement noise in each of the two measured mode shapes, if added, is different. White noise is then added to $\mathbf{Z}^{\text{num},2}$ and $\mathbf{Z}^{\text{num},4}$ to simulate measurement noise, and signal-to-noise ratios of the two mode shapes are 60 db. wMSDIs δ associated with two measured mode shapes of the second mode of the composite plate are shown in Figs. 5(a) and 5(b), where relatively high δ values can be observed beyond the delamination area, which can be regarded as disturbance caused by the measurement noise. sMSDI $\tilde{\delta}$ associated with the mode is calculated using its two δ, as shown in Fig. 5(c). Positions and lengths of upper and lower edges of the delamination area can be better identified, while disturbance caused by the measurement noise is reduced. Similar observations can be obtained from δ and $\tilde{\delta}$ associated with the fourth mode of the composite plate, as shown in Fig. 6, where positions and lengths of left and right edges of the delamination area can be better identified in $\tilde{\delta}$ than δ. aMSDI ρ associated with the two modes is then calculated using their measured mode shapes, as shown in Fig. 7, where positions and lengths of edges of the delamination area can be accurately and completely identified.

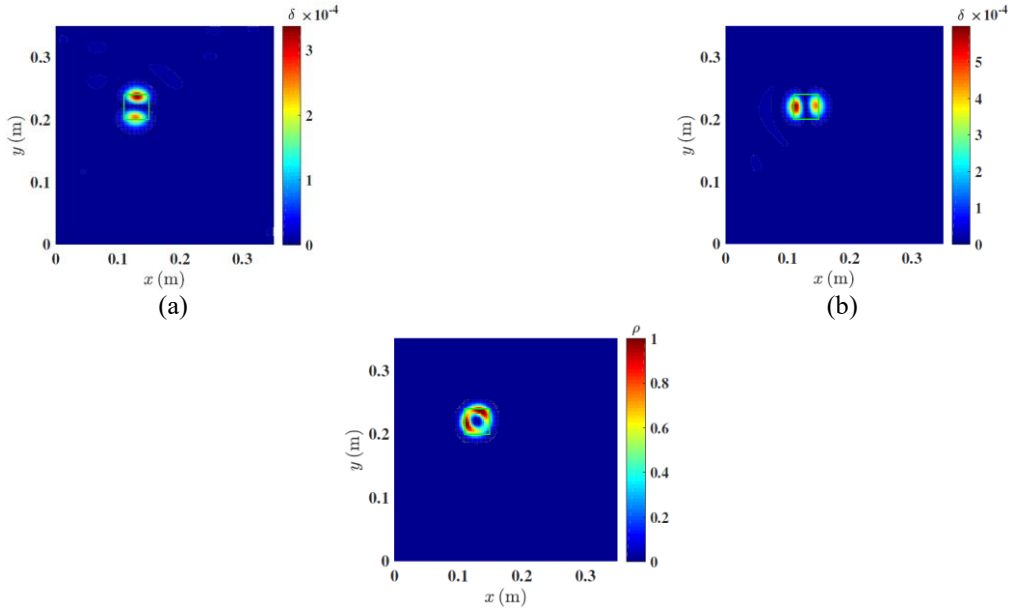

Fig. 4 wMSDIs δ associated with (a) $\mathbf{Z}^{\text{num},2}$ and (b) $\mathbf{Z}^{\text{num},4}$ of the composite plate with delamination, and (c) ρ associated with $\mathbf{Z}^{\text{num},2}$ and $\mathbf{Z}^{\text{num},4}$

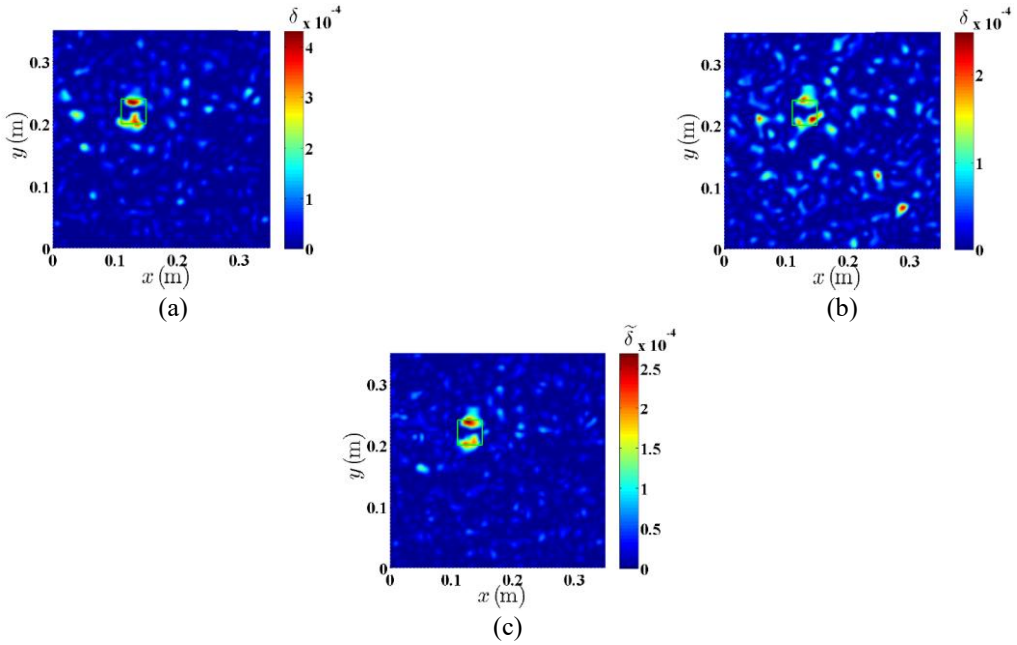

Fig. 5 (a) wMSDI δ associated with a measured mode shape of the second mode of the composite plate with measurement noise, (b) δ associated with another measured mode shape of the second mode of the composite plate with measurement noise, and (c) sMSDI $\tilde{\delta}$ associated with the second mode using two $\tilde{\delta}$ in (a) and (b)

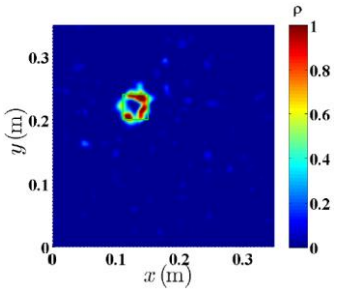

Fig. 7 aMSDI ρ using $\tilde{\delta}$ associated with the second and fourth modes of the composite plate in Figs. 5(c) and 6(c)

4. Experimental Investigation

A laminated composite plate with delamination was manufactured to experimentally investigate the proposed method. Its dimensions and material properties and dimensions of the delamination area are the same as those described in Sec. 3. The composite plate was manufactured using FS-A23 resin and FS-B412 hardener. In the composite plate, a teflon film was placed between the third and fourth laminates of the composite plate during its manufacturing process to simulate the delamination. A strip area with the width of 2.54 cm adjacent to one boundary of the composite plate was clamped by two aluminium beams with the width of 2.54 cm that were clamped by a bench vice, as shown in Fig. 8(a). Hence, a measured mode shape had a smaller size than that of the corresponding mode shape from the finite element model. Since the width of the bench vice jaw was smaller than the side length of the composite plate, the clamping force imposed on the clamped area of the composite plate was not evenly distributed along the length of the clamped area and the clamped boundary condition was imperfect. Since the proposed method isolates anomalies in mode shapes caused by delamination in composite plates, it is applicable to composite plates with any boundary conditions, such as the imperfectly clamped boundary in the experiment here, as well as those with nonlinearities. Further, use of the proposed method can be extended to structures with curved surfaces or more complicated, smooth geometries, as it inspects smoothness of a mode shape and identifies damage in neighborhoods of its anomalies being manifested in the damage indices.

In the test setup shown in Fig. 8, a speaker and a Polytec PSV-500 scanning laser Doppler vibrometer were used to excite the composite plate and measure its response, respectively. The speaker was placed so close to the plate that a measured mode shape could have a high signal-to-noise ratio; sound pressure on the plate was not measured here. Use of the non-contact acoustic excitation generated by the speaker has an advantage over those of other excitation sources that require contact with a structure, such as lead zirconate titanate (PZT) sensors, by which unwanted mass-loading effects can be eliminated. Also, equipped with the mass-loading-free feature, the vibrometer is capable of accurate vibration measurements without affecting intactness of a structure, while optical fibers, accelerometers and strain gauges need to be embedded in or attached to the structure for damage identification. The vibrometer was in the "FastScan" mode for automatic mode shape measurement. A retro-reflective tape was attached to the composite plate in order to enhance the signal-to-noise ratio of measured response by the vibrometer. Though attaching the retro-reflective tape introduced some unwanted mass loading to the plate, the loading did not adversely affect damage identification here. The reason is that effects of the mass of the retro-reflective tape on measured mode shapes were evenly distributed over the whole plate and anomalies in the mode shapes due to damage can still be isolated in the proposed damage indices. In the "FastScan" mode, a laser spot from the vibrometer stayed at a measurement point on the composite plate to measure its response for a user-defined number of periods and then moved to the next measurement point. Due to this feature, a steady-state vibration shape of the composite plate under sinusoidal excitation could be measured in a point-by-point, but automatic and rapid, manner. When the composite plate was excited at one of its natural frequencies, a measured steady-state vibration shape could be considered as its mode shape at the natural frequency. Approximate frequency response functions of the composite plate were measured, with measured velocity response of several randomly selected measurement points and a burst chirp signal given to the speaker serving as response and excitation signals, respectively. The measured frequency response functions had a frequency range from 0 to 1024 Hz with a frequency resolution of 1 Hz.

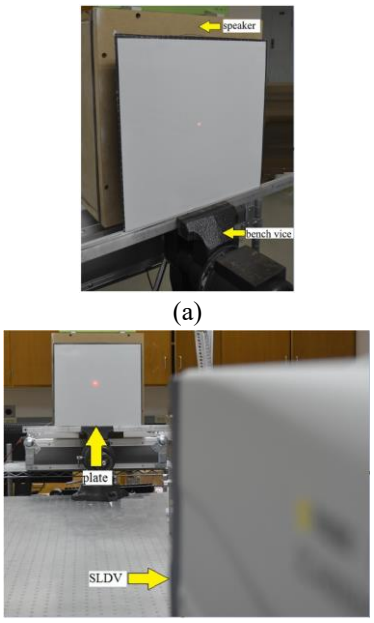

(a)

(b)

Fig. 8 (a) Fixture of the composite plate with delamination and (b) the test setup for mode shape measurement of the composite plate. SLDV in (b) stands for scanning laser Doppler vibrometer

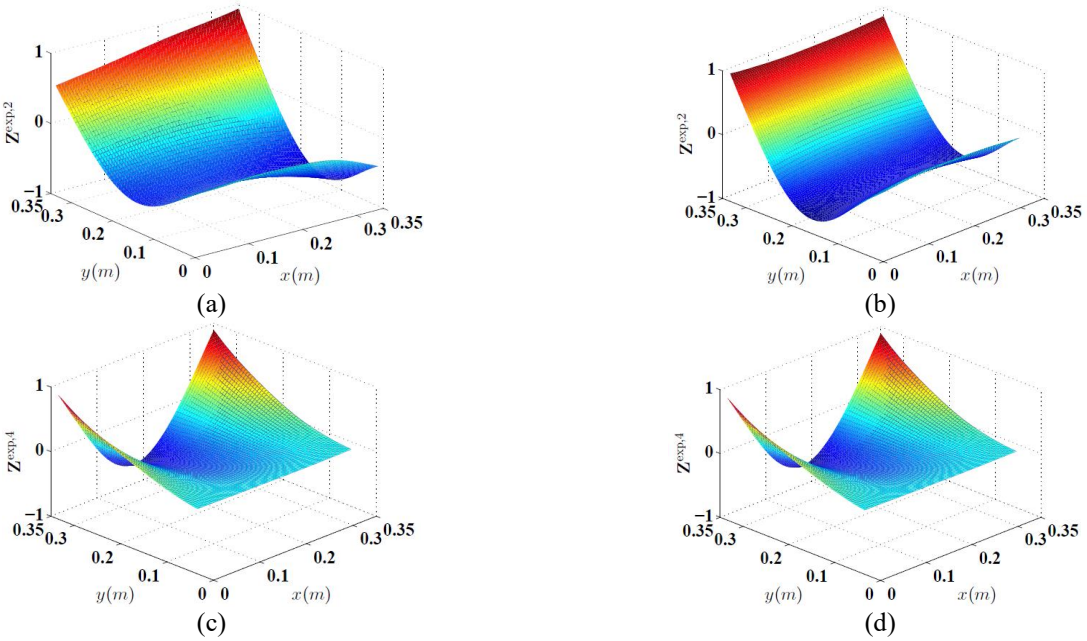

Fig. 9 Mode shape of the composite plate at 89 Hz, (b) another mode shape at 89 Hz, (c) a mode shape of the composite plate at 150 Hz, and (d) another mode shape at 150 Hz

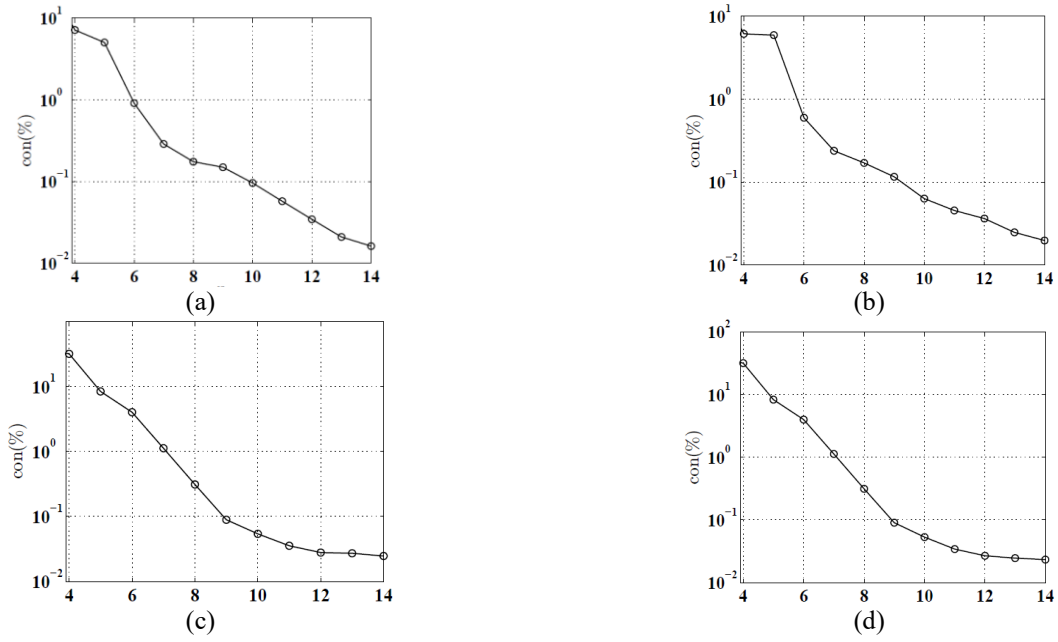

Fig. 10 (a) Convergence indices con of the mode shape at 89 Hz, (b) con of another mode shape at 89 Hz, (c) con of the mode shape at 150 Hz, and (d) con of another mode shape at 150 Hz

There were two peaks at 89 Hz and 150 Hz in a measured frequency response function. A measurement grid with 61×67 measurement points was then assigned to the composite plate to measure its mode shapes at 89 Hz and 150 Hz. Distances between adjacent measurement points in the x- and y-directions were approximately 0.005 m. Mode shapes at 89 Hz and 150 Hz are shown in Fig. 9, where each mode shape was measured twice so that δ of two mode shapes associated with each of the two frequencies can be used to yield $\tilde{\delta}$. Mode shapes at 89 Hz and 150 Hz correspond to the second and fourth modes of the composite plate in the finite element model in Sec. 3.

Convergence indices con associated with the mode shapes in Figs. 9(a) through 9(d) are shown in Figs. 10(a) through 10(d), respectively, and proper orders of

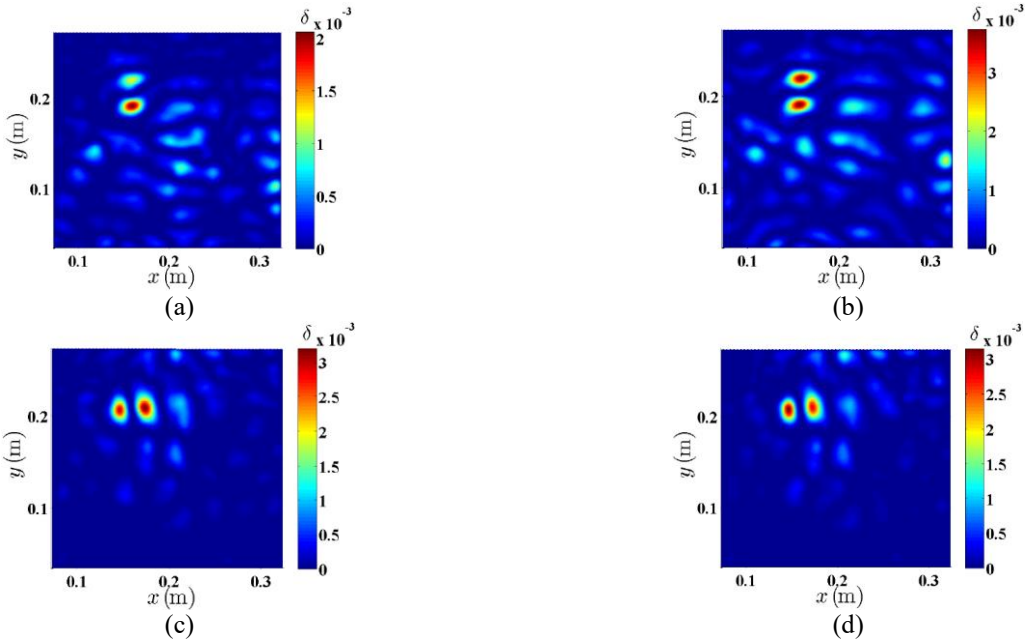

Fig. 11 (a) wMSDI δ associated with the mode shape at 89 Hz, (b) δ associated with another mode shape at 89 Hz, (c) δ associated with another mode shape at 150 Hz, and (d) δ associated with another mode shape at 150 Hz

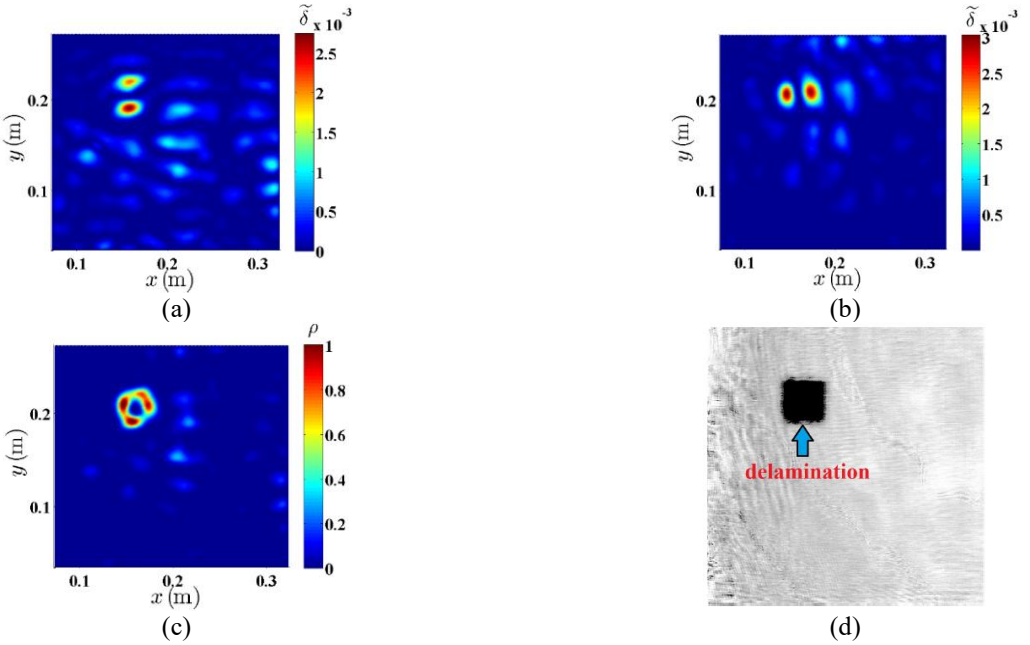

Fig. 12 (a) sMSDI $\tilde{\delta}$ associated with the two mode shapes at 89 Hz, (b) $\tilde{\delta}$ associated with the two mode shapes at 150 Hz, (c) ρ associated with $\tilde{\delta}$ in (a) and (b), and (d) a C-scan image of the composite plate with delamination

polynomial fits for the mode shapes were determined to be 12, 11, 11 and 11, respectively. Weighted MSDIs δ associated with the two mode shapes at 89 Hz and the two mode shapes at 150 Hz are shown in Fig. 11, where disturbance caused by measurement noise and error can be observed beyond the delamination area. sMSDI $\tilde{\delta}$ associated with the second and fourth modes of the composite plate are shown in Figs. 12(a) and 12(b), respectively. Similar to the identification results of the finite element model in Sec. 3, upper and lower edges of the delamination area can be identified in $\tilde{\delta}$ associated with the mode shapes at 83 Hz, and left and right edges of the delamination area can be identified in $\tilde{\delta}$ associated with the mode shapes at 150 Hz. aMSDI ρ associated $\tilde{\delta}$ in Figs. 12(a) and 12(b) is calculated, as shown in Fig. 12(c). A C-scan image of the composite plate with delamination is shown in Fig. 12(d). By comparing ρ in Fig. 12(c) and

the C-scan image in Fig. 12(d), it can be seen that positions and lengths of four edges of the delamination area can be accurately and completely identified. Furthermore, delamination identification results from $\tilde{\delta}$ and ρ in the experiment compared well with those from $\tilde{\delta}$ and ρ in the finite element model, though the clamped boundary in the experiment was imperfect. Since the proposed method isolate abnormaties in mode shapes caused by delamination in composite plates, it is applicable to composite plates with any boundary conditions, such as the imperfectly clamped boundary in the experiment, and those with nonlinearities. The proposed methodology can be further extended to identify damage in real structures with more complex geometries, such as wings of aircrafts, as it inspects for local anomaly in measured mode shapes, assuming that structures to be inspected are geometrically smooth and made of materials that have no stiffness and mass discontinuities.

5. Conclusions

An accurate non-model-based method is proposed to identify delamination in laminated composite plates using measured mode shapes. A synthetic mode shape damage index and an auxiliary mode shape damage index are formulated and positions and lengths of delamination edges can be accurately and completely identified using the damage indices. One advantage of the damage indices is that no a priori information of undamaged composite plates is needed for delamination identification, and another one is that false positive identification results due to measurement noise and error and false negative identification results due to a relatively large delamination area can be alleviated. Effectiveness of the proposed method has been numerically and experimentally investigated. Experimental delamination identification results compared well with those from a C-scan image of the composite plate, and positions and lengths of the delamination were accurately and completely identified. Robustness of the proposed method against an imperfectly clamped boundary condition of the composite plate was experimentally demonstrated. A future work can be extension of the proposed method to structures with complex geometries, such as wind turbine blades.

Acknowledgements

The authors are grateful for the financial support from the National Science Foundation under Grant Numbers CMMI-1335024, CMMI-1762917 and CMMI-1763024.

References

Castro, S. and Donadon Maurício, V. (2016), "Assembly of semi-analytical models to address linear buckling and vibration of stiffened composite panels with debonding defect", *Compos. Struct.*, **160**, 232–247.

Chakraborty, S., Mandal, B., Chowdhury, R. and Chakrabarti, A. (2016), "Stochastic free vibration analysis of laminated composite plates using polynomial correlated function expansion", *Compos. Struct*., **135**, 236-249.

Cox, I. and Gaudard, M. (2013), *Discovering partial least squares with JMP*, SAS Institute, Rockville, MD, USA.

Doebling, S., Farrar, C., Prime, M. and Shevitz, D. (1996), Damage identification and health monitoring of structural and mechanical systems from changes in their vibration characteristics: a literature review, LA-13070-MS, Los Alamos National Laboratory.

Ewins, D.J. (1984), *Modal Testing: Theory and Practice*, Research Studies Press, England.

Jafari-Talookolaei, R., Abedi, M and Hajianmaleki, M (2016), "Vibration characteristics of generally laminated composite curved beams with single through-the-width delamination", *Compos. Struct.*, **138**, 172-183.

Kim, H.Y. and Hwang, W. (2002), "Effect of debonding on natural frequencies and frequency response functions of honeycomb sandwich beams", *Compos. Struct.*, **55**(1), 51-62.

Kumar, S., Ganguli, R. and Harursampath, D. (2017), "Detecting width-wise partial delamination in the composite beam using generalized fractal dimension", *Smart Struct. Syst.*, **19**(1), 91-103.

Lestari, W., Qiao, P. and Hanagud, S. (2007), "Curvature mode shape-based damage assessment of carbon epoxy composite beams", *J. Intel. Mat. Syst. Str.*, **18**(3), 189-208.

Mendrok, K., Wojcicki, J. and Uhl, T. (2015), "An application of operational deflection shapes and spatial filtration for damage detection", *Smart Struct. Syst.*, **16**(6), 91-103.

Min, C., Kim, H., Yeu, T. and Hong, S. (2015), "Sensitivity-based damage detection in deep water risers using modal parameters: numerical study", *Smart Struct. Syst.*, **15**(2), 315-334.

Moon, T.C., Kim, H.Y. and Hwang, W. (2003), "Natural-frequency reduction model for matrix-dominated fatigue damage of composite laminates", *Compos. Struct.*, **62**(1), 19–26.

Moreno-García, P., dos Santos, J. and Lopes, H. (2014), "A new technique to optimize the use of mode shape derivatives to localize damage in laminated composite plates", *Compos. Struct.*, **108**, 548-554.

Wright, S. and Nocedal, J. (1999), *Numerical Optimization*, Springer Science, USA.

Pardoen, G. (1989), "Effect of delamination on the natural frequencies of composite laminates", *J. Compos. Mater.*, **23**(12), 1200-1215.

Qiao, P., Lu, K., Lestari, W. and Wang, J. (2007), "Curvature mode shape-based damage detection in composite laminated plates", *Compos. Struct*., **80**(3), 409-428.

Torkzadeh, P., Fathnejat, H. and Ghiasi, R. (2016), "Damage detection of plate-like structures using intelligent surrogate model", *Smart Struct. Syst.*, **18**(6), 1233-1250.

Valdes, S.H.D. and Soutis, C. (1999), "Delamination detection in composite laminates from variations of their modal characteristics", *J. Sound Vib.*, **228**(1), 1-9.

Wright, S. and Nocedal, J. (1999), *Numerical Optimization*, Springer-Verlag New York, New York, NY, USA.

Xu, Y.F. and Zhu, W.D. (2017), "Non-model-based damage identification of plates using measured mode shapes", *Struct. Health Monit.*, **16**(1), 3-23.

Xu, Y.F., Zhu, W.D. and Smith, S.A. (2017), "Non-model-based damage identification of plates using principal, mean and gaussian curvature mode shapes", *J. Sound Vib.*, **400**, 626–659.

Yang, Z., Radzienski, M., Kudela, P. and Ostachowicz, W. (2016), "Two-dimensional modal curvature estimation via Fourier spectral method for damage detection", *Compos. Struct.*, **148**, 155-167.

Yang, C. and Oyadiji, S. (2016), "Detection of delamination in composite beams using frequency deviations due to

concentrated mass loading", *Compos. Struct.*, **146**, 1-13.
Zhang, Z., Shankar, K., Morozov, E. and Tahtali, M. (2016), "Vibration-based delamination detection in composite beams through frequency changes", *J. Vib. Control*, **22**(2), 496–512.
Zou, Y., Tong, L.P.S.G. and Steven, G.P. (2000), "Vibration-based model-dependent damage (delamination) identification and health monitoring for composite structures-a review", *J. Sound Vib.*, **230**(2), 357-378.

CC